DOI: 10.1002/chem.200701841

The Rehm–Weller Experiment in View of Distant Electron Transfer

A. Rosspeintner, D. R. Kattnig, G. Angulo, S. Landgraf, and G. Grampp*[a]

Abstract: The driving-force dependence of bimolecular fluorescence quenching by electron transfer in solution, the Rehm–Weller experiment, is revisited. One of the three long-standing unsolved questions about the features of this experiment is carefully analysed here, that is, is there a diffusional plateau? New experimental quenching rates are compiled for a single electron donor, 2,5-bis(dimethylamino)-1,3-benzenedicarbonitrile, and eighteen electron acceptors in acetonitrile. The data are analysed in the framework of differential encounter theory by using an extended version of the Marcus theory to model the intrinsic electron-transfer step. Only by including the hydrodynamic effect and the solvent structure can the experimental findings be well modelled. The diffusional control region, the "plateau", reveals the inherent distance dependence of the reaction, which is shown to be a general feature of electron transfer in solution.

Keywords: differential encounter theory · electron transfer · fluorescence · Rehm–Weller plot

Introduction

Since the pioneering works of Rehm and Weller[1,2] the free-energy dependence of photo-induced electron-transfer reactions has attracted the interest of many scientists.[3–12] In fact, a multitude of so-called Rehm–Weller plots has appeared since then and stimulated the progress of electron-transfer theories and their interplay with diffusion phenomena.[13–19] Although it is a subject of ongoing controversy, the original results of Rehm and Weller have been reproduced frequently for similar systems and have posed three paradoxes: 1) no observation of the Marcus inverted region in photo-induced charge-separation reactions; 2) the lack of reversibility at small driving forces, $\Delta G_{et} \approx 0$ eV; and 3) the behaviour in the diffusional "plateau".

In detail, the predicted Marcus inverted region is often unobservable, with the quenching rates at large driving forces approaching a plateau value set by the diffusion rate constant. Although the observation of the inverted region in bimolecular charge-separation reactions has been postulated various times,[20–24] a decisive answer is still to be awaited. This behaviour is frequently modelled by a phenomenological law proposed by the original authors on the basis of the encounter complex approach in combination with an empirical model for the elementary electron-transfer reaction. The latter, unfortunately, is not derived from first principles. Several ways of overcoming the apparent "failure" of Marcus theory to consistently model Rehm's and Weller's original data, have since then been invoked.[15,25–29] Among them, the contribution of the electronically excited state of the ion-pair product is one of the most frequently argued mechanisms. This behaviour has recently been found to apply to the perylene/TCNE system.[30] Furthermore, the inclusion of the high-frequency vibrational modes is known to hamper the fall-off of the Marcus parabola in the inverted region.[31,32] This point will only give rise to a slight prolongation of the plateau region, without suppressing it completely. Indeed, the inverted region is clearly observed for charge recombination reactions with an energy gap larger than 1.5 eV, for which multichannel electron transfer is expected to contribute in just the same manner.[32–35] A great deal of recent experimental work focuses on the distance distribution of the reaction partners.[36–40] Upon increasing the reaction exergonicity, the reaction layer changes from contact to remote, whereby a high reaction rate is retained. In a recent publication, Burshtein and Ivanov[19] have point-

[a] Dr. A. Rosspeintner, D. R. Kattnig, Dr. G. Angulo,[+]
Prof. Dr. S. Landgraf, Prof. Dr. G. Grampp
Graz University of Technology
Technikerstrasse 4/I, 8010 Graz (Austria)
Fax: (+43) 316 873 8225
E-mail: grampp@tugraz.at

[+] Present address:
Institute of Physical Chemistry
Polish Academy of Sciences, Warsaw (Poland)

Supporting information for this article is available on the WWW under http://www.chemistry.org or from the author.

ed out that the consideration of this fact suffices to explain the lack of the inverted region if only a proper matrix coupling element is chosen.

The second paradox, which, however, has not received as much attention as the former, is the lack of reversibility at $\Delta G_{et} \approx 0$ eV. As a result, the Stern–Volmer constants are much higher than expected at low driving forces. As a matter of fact the reversible transfer does not work as a quenching mechanism unless an additional decay channel annihilates the reaction products. Rehm and Weller intuitively realised this issue and introduced a decay channel, which is constant with free energy and does not obey the energy-gap law. Recently, the coherent conversion to the triplet radical ion pair and its recombination to the triplet excited state of the fluorophore has been suggested as a possible mechanism for the depletion of the radical ion-pair population.[17,41] It should be noted that although this effect has not yet received experimental confirmation it allows the application of differential encounter theory (DET) to model Rehm–Weller plots consistently.[42] This is because DET is only applicable to irreversible reactions. It is interesting to note that irreversibility has also been found in systems which do not possess lower-lying triplet states.[43] Charge recombination without spin conversion can be invoked in this context.[41] This does not necessitate the recombination to the triplet state. Reversibility of the ionisation process has been proposed to be at the root of multiple Rehm–Weller plots, which were first observed by Jacques et al.[44] and recently by Porcal et al.[45] Integral encounter theory can successfully be applied in these cases.[17,41] In exciplex-forming systems, reversibility might also be more relevant than previously assumed, as recently established by magnetic field effect measurements.[46]

In this paper we focus on the plateau region of the Rehm–Weller plot, which poses the third paradox. This aspect has not previously attracted any particular interest. The research efforts have been guided by the idea that non-contact electron-transfer processes will give rise to a steady ascent over a wide range of ΔG_{et} values instead of an actual plateau. In fact, this feature is neither accounted for in Rehm's and Weller's interpolation model nor can it be explained by a contact reaction. Instead we will make use of the most advanced theory for irreversible diffusion-assisted reactions: the encounter theory in its differential version. By analysing several Rehm–Weller plots, including the original data, we show that the absence of an actual plateau constitutes a general feature, which is not unique to a particular set of data. In addition we present data for a new chemical system that holds two crucial advantages compared to previous systems: firstly, a single fluorophore is used to monitor a relatively wide diapason of exergonicity and, secondly, only quenchers of the nitroarene type are employed in the plateau region. These two factors promise a comparatively small scatter and analysis in terms of a single set of parameters for electron transfer and diffusion is better justified.

This paper is not aimed at giving a definite explanation for the lack of the Marcus inverted region, but is intended to explain the steady increase in the region formerly referred to as the diffusional plateau.

Theory

Differential encounter theory: Differential encounter theory predicts that the concentration of the excited fluorophore, $N(c,t)$, obeys Equation (1), in which τ denotes the fluorescence lifetime, c the quencher concentration and $k(t)$ is the time-dependent quenching rate. This last parameter comprises the combined effect of mutual diffusion and the elementary quenching process.

$$N(c,t) = \exp\left(-\frac{t}{\tau} - c\int_0^t k(t')\mathrm{d}t'\right) \tag{1}$$

It is related to the auxiliary quantity $n(r,t)$ by Equation (2):

$$k(t) = 4\pi\int_\sigma^\infty w(r)n(r,t)r^2\mathrm{d}r \tag{2}$$

Here $w(r)$ is the distance-dependent electron-transfer probability,[47] σ denotes the contact radius, and $n(r,t)$ is the solution of the diffusion-reaction equation [Eq. (3)]

$$\frac{\partial n(r,t)}{\partial t} = \hat{\mathcal{L}}(r)n(r,t) - w(r)n(r,t) \tag{3}$$

The operator $\hat{\mathcal{L}}(r)$ is defined by Equation (4) in which $v(r)$ denotes the effective potential due to the solvent structure (in units of k_BT), and $D(r)$ is the mutual diffusion coefficient which is a function of the interparticle distance due to hydrodynamic hindrance.[40]

$$\hat{\mathcal{L}}(r) = \frac{1}{r^2}\frac{\partial}{\partial r}r^2D(r)\exp(-v(r))\frac{\partial}{\partial r}\exp(v(r)) \tag{4}$$

Equation (3) is subject to the Boltzmann initial condition $n(r,0) = g(r) = \exp(-v(r))$, the outer boundary condition [Eq. (5)] and the reflecting inner boundary condition [Eq. (6)].[48]

$$n(r \to \infty, t) = 1 \tag{5}$$

$$\left(\frac{\partial n(r,t)}{\partial r} + n(r,t)\frac{\mathrm{d}v(r)}{\mathrm{d}r}\right)\Big|_{r=\sigma} = 0 \tag{6}$$

The steady-state fluorescence intensity is proportional to the integral of $N(c,t)$ over time, which allows the relative fluorescence intensity to be written as Equation (7)

$$\frac{I}{I_0} = \frac{\int_0^\infty N(c,t)\mathrm{d}t}{\int_0^\infty N(0,t)\mathrm{d}t} = (1 + c\kappa(c)\tau)^{-1} \tag{7}$$

For low concentrations of the quencher we obtain Equation (8) with κ_0 given by Equation (9).

$$\frac{I}{I_0} = (1 + c\kappa_0\tau)^{-1} \tag{8}$$

$$\kappa_0 = \frac{\tilde{k}(1/\tau)}{\tau} \tag{9}$$

Here $\tilde{k}$ denotes the Laplace transform of $k(t)$, which is a function of the Laplace transform of $n(r,t)$, $\tilde{n}(r,s)$. For $\tilde{n}(r,s)$, Equations (3), (5) and (6) yield Equation (10)

$$\tilde{n}(r,s) = (s + w(r) - \hat{\mathcal{L}}(r))^{-1} n(r,t=0) \tag{10}$$

Equation (10) can be solved numerically by discretising the r domain by using finite difference techniques. While the inner boundary condition can be implemented by using the particle preservation requirement, for the outer boundary we truncate the domain at finite r and make use of the asymptotic solution given in Equation (11)

$$\tilde{n}(r,s) \text{Å} 1/s + \text{const.} \cdot \exp(-r\sqrt{s/D})/r \tag{11}$$

A highly efficient computational procedure ensues, which yields the discretised $\tilde{n}(r,s)$ as a solution to a tridiagonal linear system.

Hydrodynamic effect and solvent structure: In the present study the diffusion operator, $\hat{\mathcal{L}}(r)$, includes a distance-dependent diffusion coefficient, $D(r)$, and a potential, $v(r)$, accounting for the solvent structure (cf. Figure 1). The r-dependence of the diffusion coefficient is attributed to the hydrodynamic effect, which is a consequence of the mutual hindrance of approaching donor and acceptor molecules. For small interparticle distances the diffusion coefficient is reduced substantially. The model of Deutch and Felderhof[49] gives an estimate of the effect for two solutes of equal size ($\sigma/2$), which are much larger than the solvent molecule [Eq. (12)]. In this equation $D = D(\infty)$ is the bulk diffusion coefficient.

$$D(r) = D\left(1 - \frac{3\sigma}{4r}\right) \tag{12}$$

The donor–acceptor pair distribution function $g(r)$, on the other hand, accounts for the microscopic structure of the condensed phase. For the low concentrations of quenchers used, quencher–quencher excluded volume effects[39] are negligible and $g(r)$ parallels the solvent density distribution.[40,50] The inclusion of the solvent structure leads to an increased population of quenchers in the immediate vicinity of the photo-excited fluorophore. The radial distribution function of the solvent was evaluated solving the Percus–Yevick equation.[51]

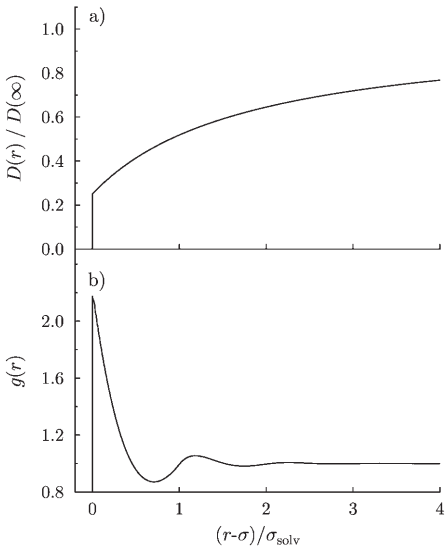

Figure 1. a) The spatial dependence of the relative diffusion coefficient, $D(r)/D(\infty)$, using the Deutch and Felderhof expression; b) the solvent structure, $g(r)$, obtained from solving the Percus Yevick equation.

Electron transfer: The intrinsic electron-transfer reaction of the quenching process is described by using Marcus theory.[52,53] For the data under investigation, which cover a wide range of free energies, the multichannel version is applied. It considers the electron transfer to numerous vibronic sublevels of the reaction products. Provision has to be taken of the saturation of the ionisation rate at short interparticle distances. In the case of extremely efficient coupling, the limiting step for the electron transfer can become the diffusional motion of the system along the reaction coordinate to the crossing point.[54–56] This so-called "dynamic solvent effect" is accounted for by including τ_L, the longitudinal relaxation time of the solvent polarisation.[57] The reaction probability for the electron transfer, $w(r)$, is then given by[30]

$$w(r) = \sum_{n=0}^{\infty} \frac{U(r)e^{-S}S^n}{n! + U(r)\tau_s e^{-S}S^n} \exp\left(-\frac{(\Delta G_{et}(r) + \lambda(r) + \hbar\omega n)^2}{4k_B T\lambda(r)}\right) \tag{13}$$

where $S = \lambda_q/(\hbar\omega)$, with ω denoting the frequency and λ_q the reorganization energy of the quantum mode.

$$U(r) = \frac{V_0^2}{\hbar}\exp\left(-\frac{2(r-\sigma)}{L}\right)\sqrt{\frac{\pi}{\lambda(r)k_B T}} \tag{14}$$

and

$$\tau_S = 4\tau_L\sqrt{\frac{\pi k_B T}{\lambda(r)}} \quad (15)$$

The distance dependencies of both the free energy, ΔG_{et}, and the outer sphere reorganisation energy, λ, are taken into account: see Equations (16) and (17) in which $r_c = e^2/(4\pi\varepsilon_0\varepsilon k_B T)$ denotes the Onsager radius.

$$\Delta G_{et}(r) = \Delta G_{et}(\sigma) - k_B T\left(\frac{r_c}{r} - \frac{r_c}{\sigma}\right) \quad (16)$$

$$\Delta G_{et}(\sigma) = E^{ox}_{1/2}(F) - E^{red}_{1/2}(Q) - E_{00} - \frac{k_B T r_c}{\sigma} \quad (17)$$

Monte Carlo simulations have shown that the classical Marcus expression does not only overestimate $\lambda(\sigma)$, but also results in a different distance dependence.[58] Henceforth we will use an approximation for $\lambda(r)$ [Eq. (18)] similar to the one which has already been successfully applied by Matsuda et al.[16]

$$\lambda(r) = \lambda(\infty) - \frac{d}{r} \quad (18)$$

in which $\lambda(\infty)$ takes on the value of the Marcus outer-sphere reorganisation energy at infinite fluorophore quencher separation [Eq. (19)], and d is a variable parameter accounting for the fact that generally the reorganisation energies at contact are found to be overestimated by the Marcus expression.

$$\lambda(\infty) = \frac{e^2}{2\pi\varepsilon_o\sigma}\left(\frac{1}{n_D^2} - \frac{1}{\varepsilon}\right) \quad (19)$$

The parameter d was set to 10.5 Å eV, giving rise to 61% of the contact value if Marcus theory was applied, which is in good agreement with previous observations.[58,59]

Results and Discussion

Figure 2 shows the steady-state quenching rate dependence on the reaction free energy for several experimental data sets (see also Table 1). Besides the data obtained in this study, we have included Rehm's and Weller's original data[1] and a representative study by Niwa et al.[60] Niwa's data spans a range of more than 2.5 eV. It is clearly observed that all three data sets follow a common trend, which is typical for this type of experiment. As expected, the scatter for the 2,5-bis(dimethylamino)-1,3-benzenedicarbonitrile (DMBCN) data is indeed smaller than that for Rehm's and Weller's original data for the reasons indicated above. Note that all data sets are characterised by a steady increase of the rate constant in the range up to approximately −2 eV, and do not level off and give rise to a plateau at a rate equal to the diffusion rate, $k_{diff} = 4\pi\sigma D$. This observation is evident when represented on a linear scale, as seen in Figure 2b. It should be noted that this feature has not yet attracted particular interest in the scientific literature, probably due to the fact that it conflicts with the predictions posed by the Rehm–Weller empirical model. In fact, the

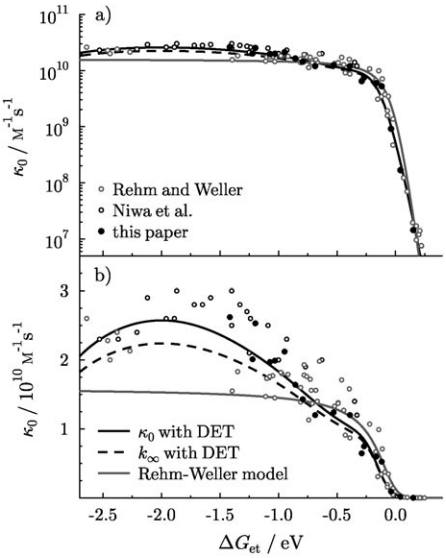

Figure 2. κ_0 versus ΔG_{et} for the original Rehm–Weller data, the data of Niwa et al., and our data. The lines show the result of fitting Weller's data with his contact model (grey line) and fitting all data simultaneously using DET with Marcus multichannel (black line), the hydrodynamic effect and the solvent structure. Additionally, the stationary rate constant, k_∞, is given as a black dashed line. a) The well-known semi-logarithmic presentation, which focuses on the ascending branch in the kinetic regime. b) An alternative linear anamorphosis emphasising the diffusional pseudo-plateau.

Table 1. Free-energy changes for the electron transfer fluorescence quenching of 2,5-bis(dimethylamino)-1,3-benzenedicarbonitrile by aromatic quenchers, ΔG_{et}, the quencher reduction potentials, $E^{red}_{1/2}$ and the low concentration fluorescence quenching rate constants, κ_0, in acetonitrile at 298.2 K.

Quencher[a]	$E^{red}_{1/2}$[b] [V]	Ref.	ΔG_{et} [eV]	κ_0 [10^9 M^{-1} s^{-1}]
14DNB	−0.67	[94]	−1.42	26
4NBN	−0.87	[94]	−1.22	20
13DNB	−0.89	[94]	−1.20	25
3NBA	−1.02	[95]	−1.07	20
Cl4NB	−1.06	[94]	−1.03	20
NB	−1.14	[94]	−0.95	21
34MNB	−1.23	[95]	−0.86	16
23MNB	−1.30	[94]	−0.79	14
26MNB	−1.40	[95]	−0.69	12
14AB	−1.56	[96]	−0.53	12
Qui	−1.70	[97]	−0.39	12
23MQui	−1.80	[95]	−0.29	6.5
BP	−1.82	[94]	−0.27	7.5
44MBP	−1.92	[98]	−0.17	6.0
4ClAP	−1.97	[99]	−0.12	5.3
44MoBP	−.05	[98]	−0.04	0.9
AP	−2.13	[99]	0.04	0.2
4MAP	−2.24	[99]	0.15	0.01

[a] For an explanation of the abbreviations of the quenchers, see the Experimental Section. [b] The data from the different references have been corrected to refer to SCE_{aq} in acetonitrile.

latter anticipates an actual plateau with an invariant quenching rate equal to the diffusion rate. It should be pointed out that Rehm's and Weller's equation is merely an empirical model that is not based on first principles. Instead it appeared to be "the most reasonable function" for a monotonous dependence of the free energy of activation, ΔG^*, on the reaction free energy, ΔG_{et}, according to the original authors. Qualitatively it appears as if the quenching rate constant, κ_0, was faster than the diffusion rate, k_{diff}, over a wide range of driving forces. In a simplistic contact model this is tantamount to an increase of the effective quenching radius. Within the differential encounter theory employed here the phenomenon is not at all surprising and can be rationalised by a shift of the initial distribution of ions,[37,42] $m_0(r)$, away from contact. This behaviour is a direct consequence of the intrinsic distance dependence of the electron transfer rate, $w(r)$, and the diffusive approach of the reactants. In fact, $w(r)$ assumes its maximum at contact for small values of ΔG_{et}, although there are peaks at distances larger than the contact distance for driving forces larger than 1.2 eV (see Figure 3). In Figure 3, the maximum of $w(r)$ is indicated by a thick solid line. This fact can also be appreciated from the contour plot. In combination with the diffusive nature of the encounter, $w(r)$ determines the location of the electron transfer and thus the initial distribution of ions. It is evident from Figure 4 that an appreciable number of ions is born at distances as large as $\sigma+6$ Å. The functional dependence closely mirrors the actual quenching rate as is obvious from a comparison of Figures 2b and 4. Because the three data sets compiled in Figure 2 show the same overall trend we attempted a simultaneous fit using differential encounter theory and the rate model introduced in the section above on electron transfer. This approach is guided by the idea of working out a common basis that is more significant than the variation between the systems. While the necessity to include the solvent structure and the hydrodynamic effect in the theoretical models has been demonstrated clearly for highly viscous solvent systems,[37,50] these issues have not attracted attention in the analysis of Rehm–Weller plots. In order to evaluate the impact of these refinements of the theoretical model we analysed the quenching data including: 1) solvent structure and the hydrodynamic effect; 2) only the hydrodynamic effect; 3) only the solvent structure; 4) neither the solvent structure nor the hydrodynamic effect. For all models only the coupling matrix element, V_0, and its characteristic decay length, L, were adjusted. In addition, the following parameter values were adopted:

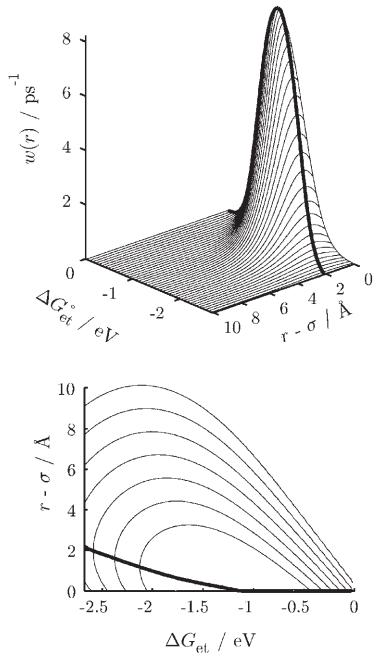

Figure 3. Plot of the reaction probability for electron transfer, $w(r)$, as a function of the free energy of electron transfer, ΔG_{et}, and the interparticle distance, $r-\sigma$. The lower panel shows the contour plot of the data. The contour levels are equally spaced on a logarithmic scale. The thick solid line marks the position of the maximum as a function of ΔG_{et}.

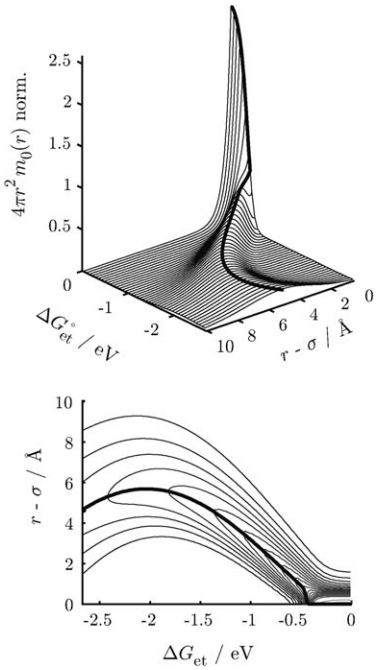

Figure 4. Plot of the normalised initial ion distribution, $4\pi r^2 m_o(r)$, as a function of the free energy of electron transfer, ΔG_{et}, and the interparticle distance, $r-\sigma$, at a quencher concentration of 5×10^{-3} M. The lower panel shows the contour plot of the data. The reaction changes from being totally contact in the kinetic regime ($\Delta G_{et} > -0.5$ eV) to totally remote in the diffusion regime ($\Delta G_{et} < -0.5$ eV). The thick solid line marks the position of the maximum as a function of ΔG_{et}.

$\sigma = 6.5$ Å	$D = 300$ Å^2 ns^{-1}
$\eta = 0.28$	$\sigma_{solv} = 3.62$ Å
$\lambda_q = 0.42$ eV	$\hbar\omega = 0.186$ eV
$S = 2.26$	$\tau_L = 0.17$ ps
$\varepsilon = 35.9$	$n_D = 1.344$

The parameters ε and n_D were taken from reference [61]. The value of 0.186 eV (corresponding to 1500 cm^{-1}) for the

energy of the quantum mode, $\hbar\omega$, has previously been found to be applicable.[62–64] This parameter corresponds to the mean value of the high frequency quantum mode contributing to the electron-transfer reaction. For aromatic compounds similar to those used here, it has been argued to be close to the C=C stretching mode in the ring. λ_q was estimated as the mean overall inner reorganisation energy calculated on the basis of Nelsen's method.[65] The value of the electron-phonon coupling strength, S, has been calculated as $\lambda_q/(\hbar\omega)$,[66] and yields a value corresponding to a middle-strong coupling, in accordance with Levich[67] and many others.[16,30,68,69] $\tau_L=\tau_D n_D^2/\varepsilon$, in which the value for τ_D was taken from reference [70]. The solvent diameter, σ_{solv}, was taken from reference [71] and the packing fraction, $\eta = \frac{\pi\rho_m\sigma_{solv}^3 N_A}{6M_w}$, calculated from the mass density ρ_m, and the molar weight, M_w, where N_A denotes Avagadro's number. The diffusion coefficient used is in perfect agreement with those used in other works employing the same solvent.[16,19,30,63]

However, other choices of electron-transfer parameters are frequent in the literature and do not give rise to substantially different results. In the Supporting Information some of these parameter sets are presented and rationalised. The reader should note that a comparison of many different systems is inherent in the Rehm–Weller plot and thus the preference for one parameter set over the other is difficult to argue. Nevertheless, the conclusions obtained in this work are to a large extent independent of the actual parameters used, always assuming that these are chosen within the bounds of physical reasonability.

In Figure 2 we also included the stationary rate constant, k_∞. This is the rate attained for the steady-state pair distribution of the quenchers about the excited fluorophore. It is evident that for all rates in the diffusion regime, k_∞ underestimates the low concentration Stern–Volmer constant, κ_0. In particular, at large driving forces the quenching is governed by the transient term (non-stationary diffusion). From this it is inferred that treatments that base their analysis on k_∞, as, for example, those derived from the closure approximation by Tachiya, can not be applied to steady-state data like ours.[72] Furthermore, the relative contribution of the non-stationary quenching does depend on the fluorophore lifetime. For this work we took $\tau=22$ ns (DMBCN). However, using 14 ns, which is more appropriate for the data by Niwa et al., yields very similar results. In contrast, significantly shorter lifetimes may give rise to an underestimation of κ_0 with respect to that calculated here.

Table 2 summarises the fit results obtained for the four models. Note that the inclusion of the hydrodynamic effect gives rise to a significant improvement of the fit as judged from the relative residual norm. The fits that do not account for the hydrodynamic effect overshoot the experimental data in the range from -0.5 to -1.0 eV. Thus its inclusion is clearly justified. The goodness of fit alone does not substantiate the inclusion of the solvent structure. However, only by including these two effects simultaneously can a simulation with quite a small value of the effective coupling matrix element, $V_{eff}=V_0\sqrt{e^{-S}S^n/n!}$,[73] be achieved. Not accounting for these effects, on the other hand, gives rise to a large coupling matrix element, which renders the applicability of the electron-transfer model questionable.[74] Indeed, making use of large V_{eff}, Matsuda et al.[16] obtained results similar to that of model 4, in which the solvent structure and the hydrodynamic effect are not taken into account. In summary, model 1 provides the most consistent description of the experimental trends, while simultaneously obeying the limitations of the applied electron transfer model. Actually, the fit parameter L is typical for this kind of system and agrees well with the values suggested in references [75] and [76]. Note that the decay length deduced from the Marcus rate expression is expected to exceed that determined on the basis of an exponential model,[77,78] as has been shown in references [75,79]. Note that V_0 and L are certainly slightly correlated, as can be appreciated from the error surface given in the Supporting Information. The deviation from Marcus' proposal for the distance dependence of λ is mandatory to reproduce the experimental data in the range above -0.5 eV. A similar result could be obtained by including an additional reaction channel at low exergonicities, as has been shown in reference [80].

Table 2. Comparison of the four models used to describe the three sets of quenching data. The fitting parameters were the coupling matrix element, V_0, and its decay length, L. The maximal effective coupling matrix element, V_{eff}, is additionally given. The optimisation criterion (opt. crit.) was evaluated from $\Sigma_i((\kappa_{0,i}-\kappa_{0,fit,i})/\kappa_{0,i})^2$, in which $\kappa_{0,i}$ denotes the experimental value and $\kappa_{0,fit,i}$ its theoretical counterpart.

	hydrodynamic hindrance	solvent structure	L [Å]	V_0 [meV]	V_{eff} [meV]	opt. crit.
1	yes	yes	2.0	52	27	6.6
2	yes	no	1.6	117	60	6.5
3	no	yes	1.1	53	27	10.9
4	no	no	0.2	1000[a]	520	10.7

[a] The value corresponds to the upper bound allowed in the optimisation procedure.

Experimental Section

2,5-Bis(dimethylamino)-1,3-benzenedicarbonitrile (DMBCN, $E_{1/2}^{ox}=0.73$ V,[81] $E_{00}=2.76$ eV[82], $\tau=22$ ns) was synthesised and purified as described in reference [81]. 1,4-Dinitrobenzene (14DNB, Aldrich, 98%), 4-nitrobenzonitrile (4NBN, Fluka, 98%), 1,3-dinitrobenzene (13DNB, Schuchardt), 3-nitrobenzaldehyde (3NBA, Aldrich, 99%), 1-chloro-4-nitrobenzene (Cl4NB, Aldrich, 99%), quinoxaline (Qui, Fluka, 97%), 2,3-dimethylquinoxaline (23MQui, Aldrich, 97%), 4,4′-dimethylbenzophenone (44MBP, Fluka, >98%) and 4,4′-dimethoxybenzophenone (44MoBP, Schuchardt, 98%) were purified by sublimation. Nitrobenzene (NB, Fluka, 99.5%), 2,3-dimethylnitrobenzene (23MNB, Aldrich, 99%), 2,6-dimethylnitrobenzene (26MNB, Aldrich, 99%), 4-chloroacetophenone (4ClAP, Fluka, 97%) and 4-methylacetophenone (4MAP, Fluka, 95%) were purified by distillation. 3,4-dimethylnitrobenzene (34MNB, Aldrich, 99%), 1,4-diacetylbenzene (14AB, Aldrich, 99%), benzophenone (BP, Fluka, >99%) and acetophenone (AP, Fluka, 99%) were used as received. Acetonitrile (Merck, isocratic grade) was dynamically dried over a molecular sieve (3 Å).

Absorption spectra were recorded on a Shimadzu UV-3101PC UV-VIS-NIR spectrophotometer. Fluorescence spectra were recorded on a Jobin–

Yvon Spex FluoroMax-2 spectrofluorimeter. Time-resolved measurements were performed using a home-built single-photon timing setup described in reference [83], with a 450 nm LED (Picoquant, FWHM 0.7 ns) as the excitation light source.

The measurements were carried out in septa-sealed quartz cuvettes (10 mm Suprasil glass) and the solutions were purged with Ar for 15 min prior to measurement. The sample invariability with respect to changes in concentration in this procedure was checked by recording absorption spectra before and after the procedure. The concentration of the fluorophore was chosen such that the absorption at the excitation wavelength (430 to 440 nm) did not exceed 0.1, corresponding to a maximum concentration of 3×10^{-5} M. The quencher concentrations were chosen such that the observed Stern–Volmer plots did not show deviations from linearity, thus being smaller than 10^{-2} M for the diffusion limited reactions. All experiments were performed at (25 ± 1)°C.

Conclusions

By using a single fluorophore (DMBCN) a Rehm–Weller plot has been constructed. The ascending behaviour in the "plateau region" has been analysed in detail and shown to be universally observable by comparison to previous data. In particular, Rehm's and Weller's original data have been revisited and found to show analogous behaviour. The ΔG_{et} dependence of the quenching rate originates from the distance dependence of the intrinsic electron-transfer rate in combination with diffusion in the effective potential due to the solvent structure. Unlike previous studies that tried to explain this kind of experiment, we achieved a fit using a set of parameters that are within the limits of applicability of a physically grounded theoretical model.

We note that the individual parameter values are not essential, but rather the general shape of the intrinsic rate of electron transfer, $w(r)$. Evidently there are several physically reasonable parameter sets that give rise to approximately the same functional dependence. This paper is not intended to provide a parameter set, or to establish a value of any of them as the best one. This paper is about the ability of a kinetic model that includes several well-grounded physical phenomena to explain a series of experiments.

By taking into account the solvent structure and hydrodynamic hindrance, the extracted electron-transfer parameters do not exceed the limit of applicability of the electron-transfer model. More precisely, the coupling matrix element obeys $V_{eff}\leq k_BT$. The solvent structure allows the realisation of large rates in the kinetic regime without pushing the limits of the applied model too far. The non-plateau behaviour is recognised as a feature of the interplay of the individual distance dependences of the solvent reorganisation energy, the driving force, the diffusion coefficient and the solvent structure. These distance effects are clearly shown to influence the quenching process, even though the viscosity is low and non-Markovian effects are not expected to have as much relevance as in more viscous solvents.[76] On the other hand, interpolation equations, which are based on rather artificial relations between rate constant and driving force, as, for example, Rehm's and Weller's original model, as well as contact models, are recognised as being inappropriate. Unfortunately, these unphysical models continue to be in widespread use.[84–88] Indeed, the assumption of a distant electron-transfer process is mandatory to rationalise the Rehm–Weller plot from first principles.

The reader should note that the distant electron-transfer model employed here is not at all in contradiction with the observation of ultrafast charge recombination of the ions, as has been suggested by Vauthey et al.[89,90] Indeed, at the large quencher concentration employed by these authors the majority of the ions are formed through static quenching at contact. In fact, the distribution of ions then mirrors the combined effect of the solvent structure and the intrinsic rate with a large portion of ions being generated at contact. This has also been shown by Weidemaier et al.[91]

Despite these achievements one issue about the Rehm–Weller experiment remains open: the ascending branch has been rationalized assuming total irreversibility; that is, recombination to the excited state has been neglected explicitly. This is equivalent to considering a fast deactivation channel of the ions, which, however, cannot be specified any further in the present study. Two possible channels are rational: fast charge recombination to the ground state, even in the inverted region, or recombination to the triplet state following spin conversion.

The former channel has some precedents when contact complexes are considered. The first (static) quenching stage can be extraordinarily fast due to a very large matrix coupling element, V_{eff}, of dynamic nature, which is favoured by a structure existing prior to excitation.[92,93] This proposition could explain two of the Rehm–Weller paradoxes: the very fast deactivation channel in the ascending branch of the RW plot, as well as the large rate constant of the quenching at very large driving forces.

The latter channel is feasible for the present organic systems, since the reaction proceeds from a singlet excited state, higher in energy than the triplet. As a consequence the ions in the low exergonicity region will lie above the triplets as well. Note that the present analysis accommodates without restraints even the points at extremely negative ΔG_{et} values, that is, the tetracyanoethylene (TCNE) points of the original data set. The only exception is the point at largest driving force (naphthalene/TCNE), which, however, does not follow the trend of the other points at comparable driving forces. Our analysis does not assume an effective coupling matrix element that significantly exceeds k_BT, contrary to references [16] (V_{eff} at contact equals 64 meV in channels 2 and 3) and [72]. Additionally, it is not required to include the excited state of the reaction products, as has been done in reference [30] and has already been suggested by Rehm and Weller. While this cannot be viewed as definite proof against any of these suggestions, it again sheds light on the inclusion of the solvent structure for this kind of analysis.

Almost forty years of debate have led to several models explaining the ΔG_{et} dependence of photo-induced electron-transfer reactions involving freely moving particles in solution. However, the issue cannot at all be regarded as con-

cluded. Even the availability of kinetic methods able to follow chemical reactions in real time, or the theoretical deduction of theories for diffusion influenced reactions from physical principles, have thus far not been capable of resolving all the paradoxes posed by this ancient experiment. It is surprising, nearly forty years after the original experiment, so many questions remain open.

[1] D. Rehm, A. Weller, *Ber. Bunsen-Ges.* **1969**, *73*, 834–839.
[2] D. Rehm, A. Weller, *Isr. J. Chem.* **1970**, *8*, 259–271.
[3] G. J. Kavarnos, N. J. Turro, *Chem. Rev.* **1986**, *86*, 401–449.
[4] M. R. Wasielewski, *Chem. Rev.* **1992**, *92*, 435–461.
[5] B. Paulson, K. Pramod, P. Eaton, G. Closs, J. R. Miller, *J. Phys. Chem.* **1993**, *97*, 13042–13045.
[6] P. F. Barbara, T. J. Meyer, M. A. Ratner, *J. Phys. Chem.* **1996**, *100*, 13148–13168.
[7] S. J. Formosinho, L. G. Arnaut, R. Fausto, *Prog. React. Kinet.* **1998**, *23*, 1–90.
[8] S. M. Hubig, J. K. Kochi, *J. Am. Chem. Soc.* **1999**, *121*, 1688–1694.
[9] P. Jacques, X. Allonas, D. Burget, E. Haselbach, P.-A. Muller, A.-C. Sergenton, H. Galliker, *Phys. Chem. Chem. Phys.* **1999**, *1*, 1867–1871.
[10] G. P. Zanini, H. A. Montejano, C. M. Previtali, *J. Photochem. Photobiol. A* **2000**, *132*, 161–166.
[11] P. Finckh, H. Heitele, M. Volk, M. E. Michel-Beyerle, *J. Phys. Chem.* **1988**, *92*, 6585–6592.
[12] I. R. Gould, D. Ege, J. E. Moser, S. Farid, *J. Am. Chem. Soc.* **1990**, *112*, 4290–4301.
[13] N. Mataga, Y. Kanda, T. Asahi, H. Miyasaka, T. Okada, T. Kakitani, *Chem. Phys.* **1988**, *127*, 239–248.
[14] S. Nishikawa, T. Asahi, T. Okada, N. Mataga, T. Kakitani, *Chem. Phys. Lett.* **1991**, *185*, 237–243.
[15] M. Tachiya, S. Murata, *J. Phys. Chem.* **1992**, *96*, 8441–8444.
[16] N. Matsuda, T. Kakitani, T. Denda, N. Mataga, *Chem. Phys.* **1995**, *190*, 83–95.
[17] A. I. Burshtein, K. L. Ivanov, *Phys. Chem. Chem. Phys.* **2002**, *4*, 4115–4125.
[18] N. Mataga, H. Chosrowjan, S. Taniguchi, *J. Photochem. Photobiol. C* **2005**, *6*, 37–79.
[19] A. I. Burshtein, A. I. Ivanov, *Phys. Chem. Chem. Phys.* **2007**, *9*, 396–400.
[20] C. Creutz, N. Sutin, *J. Am. Chem. Soc.* **1977**, *99*, 241–243.
[21] J.-M. Chen, T.-I. Ho, C.-Y. Mou, *J. Phys. Chem.* **1990**, *94*, 2889–2896.
[22] D. M. Guldi, P. Nets, K.-D. Asmus, *J. Phys. Chem.* **1994**, *98*, 4617–4621.
[23] C. Turro, J. M. Zaleski, Y. M. Karabatsos, D. G. Nocera, *J. Am. Chem. Soc.* **1996**, *118*, 6060–6067.
[24] D. R. Worrall, S. L. Williams, F. Wilkinson, *J. Phys. Chem. B* **1997**, *101*, 4709–4716.
[25] T. Kakitani, N. Mataga, *Chem. Phys.* **1985**, *93*, 381–397.
[26] T. Kakitani, N. Mataga, *J. Phys. Chem.* **1987**, *91*, 6277–6285.
[27] G. Greiner, P. Pasquini, R. Weiland, H. Orthwein, H. Rau, *J. Photochem. Photobiol. A* **1990**, *51*, 179–195.
[28] P. Suppan, *Top. Curr. Chem.* **1992**, *163*, 95–130.
[29] G. Grampp, *Angew. Chem.* **1993**, *105*, 724–726; *Angew. Chem. Int. Ed. Engl.* **1993**, *32*, 691–693.
[30] V. Gladkikh, A. I. Burshtein, G. Angulo, S. Pages, B. Lang, E. Vauthey, *J. Phys. Chem. A* **2004**, *108*, 6667–6678.
[31] E. Buhks, M. Bixon, J. Jortner, G. Navon, *J. Phys. Chem.* **1981**, *85*, 3759–3762.
[32] J. R. Miller, L. T. Calcaterra, G. L. Closs, *J. Am. Chem. Soc.* **1984**, *106*, 3047–3049.
[33] P. Chen, S. L. Mecklenburg, T. J. Meyer, *J. Phys. Chem.* **1993**, *97*, 13126–13131.
[34] T. Asahi, M. Ohkohchi, N. Mataga, *J. Phys. Chem.* **1993**, *97*, 13132–13137.
[35] G. Grampp, G. Hetz, *Ber. Bunsen-Ges.* **1992**, *96*, 198–200.
[36] L. Burel, M. Mostafavi, S. Murata, M. Tachiya, *J. Phys. Chem. A* **1999**, *103*, 5882–5888.
[37] A. Rosspeintner, D. R. Kattnig, G. Angulo, S. Landgraf, G. Grampp, A. Cuetos, *Chem. Eur. J.* **2007**, *13*, 6474–6483.
[38] A. A. Neufeld, A. I. Burshtein, G. Angulo, G. Grampp, *J. Chem. Phys.* **2002**, *116*, 2472–2479.
[39] R. C. Dorfman, M. D. Fayer, *J. Chem. Phys.* **1992**, *96*, 7410–7422.
[40] S. F. Swallen, K. Weidemaier, M. D. Fayer, *J. Chem. Phys.* **1996**, *104*, 2976–2986.
[41] A. I. Burshtein, K. L. Ivanov, *J. Phys. Chem. A* **2001**, *105*, 3158–3166.
[42] A. I. Burshtein, *Adv. Chem. Phys.* **2000**, *114*, 419–587.
[43] A. Kapturkiewicz, P. Szrebowaty, G. Angulo, G. Grampp, *J. Phys. Chem. A* **2002**, *106*, 1678–1685.
[44] P. Jacques, X. Allonas, *J. Photochem. Photobiol. A* **1994**, *78*, 1–5.
[45] G. Porcal, S. J. Bertolotti, C. M. Previtali, M. V. Encinas, *Phys. Chem. Chem. Phys.* **2003**, *5*, 4123–4128.
[46] D. Kattnig, A. Rosspeintner, G. Grampp, *Angew. Chem.* **2008**, *120*, 974–976; *Angew. Chem. Int. Ed.* **2008**, *47*, 960–962.
[47] R. A. Marcus, P. Siders, *J. Phys. Chem.* **1982**, *86*, 622–630.
[48] Z. Schulten, K. Schulten, *J. Chem. Phys.* **1977**, *66*, 4616–4634.
[49] J. Deutch, B. U. Felderhof, *J. Chem. Phys.* **1973**, *59*, 1669–1671.
[50] S. F. Swallen, K. Weidemaier, H. L. Tavernier, M. D. Fayer, *J. Phys. Chem.* **1996**, *100*, 8106–8117.
[51] L. Tsang, J. A. Kong, K.-H. Ding, C. O. Ao, *Scattering of Electromagnetic Waves, Numerical Simulations*, 1st ed., Wiley-Interscience, New York, **2001**.
[52] R. A. Marcus, *J. Chem. Phys.* **1956**, *24*, 979–989.
[53] R. A. Marcus, *J. Chem. Phys.* **1957**, *26*, 867–871.
[54] A. I. Burshtein, A. G. Kofman, *Chem. Phys.* **1979**, *40*, 289–300.
[55] B. I. Yakobson, A. I. Burshtein, *Chem. Phys.* **1980**, *49*, 385–395.
[56] L. Zusman, *Chem. Phys.* **1980**, *49*, 295–304.
[57] V. Gladkikh, A. I. Burshtein, I. Rips, *J. Phys. Chem. A* **2005**, *109*, 4983–4988.
[58] Y. Enomoto, T. Kakitani, A. Yoshimori, Y. Hatano, M. Saito, *Chem. Phys. Lett.* **1991**, *178*, 235–240.
[59] E. H. Yonemoto, G. B. Saupe, R. H. Schmehl, S. M. Hubig, R. L. Riley, B. L. Iverson, T. E. Mallouk, *J. Am. Chem. Soc.* **1994**, *116*, 4786–4795.
[60] T. Niwa, K. Kikuchi, N. Matsusita, M. Hayashi, T. Katagiri, Y. Takabashi, T. Miyashi, *J. Phys. Chem.* **1993**, *97*, 11960–11964.
[61] J. A. Riddick, W. B. Bunger, T. K. Sakano, *Organic Solvents. Physical Properties and Methods of Purification, Vol. II of Techniques of Chemistry*, 4th ed., Wiley-Interscience, New York, **1986**.
[62] G. L. Closs, L. T. Calcaterra, N. J. Green, K. W. Penfield, J. R. Miller, *J. Phys. Chem.* **1986**, *90*, 3673–3683.
[63] T. Inada, K. Kikuchi, Y. Takahashi, T. Miyashi, *J. Phys. Chem. A* **2002**, *106*, 4345–4349.
[64] O. Nicolet, E. Vauthey, *J. Phys. Chem. A* **2003**, *107*, 5894–5902.
[65] S. F. Nelsen, S. C. Blackstock, Y. Kim, *J. Am. Chem. Soc.* **1987**, *109*, 677–682.
[66] N. R. Kestner, J. Logan, J. Jortner, *J. Phys. Chem.* **1974**, *78*, 2148–2166.
[67] V. Levich, *Adv. Electrochem. Electrochem. Eng.* **1966**, *4*, 249–371.
[68] E. Vauthey, *J. Phys. Chem. A* **2001**, *105*, 340–348.
[69] V. Gladkikh, A. I. Burshtein, S. V. Feskov, A. I. Ivanov, E. Vauthey, *J. Chem. Phys.* **2005**, *123*, 244510.
[70] Y. Marcus, *The Properties of Solvents, Wiley Series in Solution Chemistry*, Wiley, New York, **1998**.
[71] H. L. Tavernier, M. M. Kalashnikov, M. D. Fayer, *J. Chem. Phys.* **2000**, *113*, 10191–10201.
[72] G. L. Hug, B. Marciniak, *J. Phys. Chem.* **1995**, *99*, 1478–1483.
[73] J. Jortner, M. Bixon, *J. Chem. Phys.* **1988**, *88*, 167–170.
[74] A. Barzykin, P. Frantsuzov, K. Seki, M. Tachiya, *Adv. Chem. Phys.* **2002**, *123*, 511–616.

[75] V. S. Gladkikh, A. I. Burshtein, H. L. Tavernier, M. D. Fayer, *J. Phys. Chem. A* **2002**, *106*, 6982–6990.
[76] G. Angulo, G. Grampp, A. A. Neufeld, A. I. Burshtein, *J. Phys. Chem. A* **2003**, *107*, 6913–6919.
[77] A. Ponce, H. B. Gray, J. R. Winkler, *J. Am. Chem. Soc.* **2000**, *122*, 8187–8191.
[78] H. B. Gray, J. R. Winkler, *Proc. Natl. Acad. Sci. USA* **2005**, *102*, 3534–3539.
[79] A. I. Burshtein, *Adv. Chem. Phys.* **2004**, *129*, 105–418.
[80] S. Iwai, S. Murata, M. Tachiya, *J. Chem. Phys.* **2001**, *114*, 1312–1318.
[81] G. Schwarzenbacher, B. Evers, I. Schneider, A. de Raadt, J. Besenhard, R. Saf, *J. Mater. Chem.* **2002**, *12*, 534–539.
[82] A. Rosspeintner, G. Angulo, M. Weiglhofer, S. Landgraf, G. Grampp, *J. Photochem. Photobiol. A* **2006**, *183*, 225–235.
[83] S. Landgraf, *Spectrochim. Acta Part A* **2001**, *57*, 2029–2048.
[84] R. Ballardini, G. Varani, M. T. Indelli, F. Scandola, V. Balzani, *J. Am. Chem. Soc.* **1978**, *100*, 7219–7223.
[85] M. P. Scannell, G. Prakash, D. E. Falvey, *J. Phys. Chem. A* **1997**, *101*, 4332–4337.
[86] S. M. Bonesi, R. Erra-Balsells, *J. Chem. Soc. Perkin Trans. 2* **2000**, 1583–1595.
[87] M. Dossot, D. Burget, X. Allonas, P. Jacques, *New J. Chem.* **2001**, *25*, 194–196.
[88] M. F. Broglia, S. G. Bertolotti, C. M. Previtali, *J. Photochem. Photobiol. A* **2005**, *170*, 261–265.
[89] S. Pages, B. Lang, E. Vauthey, *J. Phys. Chem. A* **2004**, *108*, 549–555.
[90] E. Vauthey, *J. Photochem. Photobiol. A* **2006**, *179*, 1–12.
[91] K. Weidemaier, H. L. Tavernier, S. F. Swallen, M. D. Fayer, *J. Phys. Chem. A* **1997**, *101*, 1887–1902.
[92] E. W. Castner, D. Kennedy, R. J. Cave, *J. Phys. Chem. A* **2000**, *104*, 2869–2885.
[93] P. O. J. Scherer, M. Tachiya, *J. Chem. Phys.* **2003**, *118*, 4149–4156.
[94] H. Shalev, D. H. Evans, *J. Am. Chem. Soc.* **1989**, *111*, 2667–2674.
[95] L. Meites, P. Zuman, *CRC Handbook Series in Electrochemistry, Vol. I–V*, CRC, Boca Raton, **1977–1982**.
[96] P. J. Wagner, R. J. Truman, A. E. Puchalski, R. Wake, *J. Am. Chem. Soc.* **1986**, *108*, 7727–7738.
[97] S. Millefiori, *J. Heterocycl. Chem.* **1970**, *7*, 145–149.
[98] R. O. Loutfy, R. O. Loutfy, *J. Phys. Chem.* **1972**, *76*, 1650–1655.
[99] R. O. Loutfy, R. O. Loutfy, *J. Phys. Chem.* **1973**, *77*, 336–339.

Received: November 22, 2007
Revised: February 19, 2008
Published online: May 28, 2008

